Available online at www.sciencedirect.com
SCIENCE DIRECT®
International Journal of Mass Spectrometry 233 (2004) 373–384
International Journal of Mass Spectrometry
www.elsevier.com/locate/ijms

Mode-selective stereomutation tunneling and parity violation in $HOClH^+$ and H_2Te_2 isotopomers

Michael Gottselig, Martin Quack*, Jürgen Stohner[1], Martin Willeke

Physical Chemistry, ETH Zürich, CH-8093 Zurich, Switzerland

Received 13 January 2004; accepted 14 January 2004

Dedicated to Tilmann Märk on the occasion of his 60th birthday.

Abstract

We investigate the stereomutation tunneling processes in the axially chiral prototype ion $HOClH^+$ and in H_2Te_2 isotopomers in their relation to parity violation using quantum chemical calculations including our recently developed MC-LR approach to electroweak quantum chemistry and the quasiadiabatic channel reaction path Hamiltonian (RPH) approach. All the molecules dealt with here exhibit intermediate barriers to stereomutation (in the range from 0.1 to 0.3 eV depending on the molecule and *cis*- or *trans*-type of transition structure considered). Whereas tunneling dominates the quantum dynamics of stereomutation in all isotopomers of $HOClH^+$, the ground-state torsional tunneling splittings for hydrogen ditelluride isotopomers D_2Te_2 and T_2Te_2 are calculated to be much smaller than the parity violating energy differences ΔE_{pv} between the enantiomers of these molecules. We present a systematic investigation of the dependence of tunneling splittings upon the excitation of various vibrational modes and we identify some strongly promoting and some weakly inhibiting modes as well as essentially inactive modes. A comparison of the new results for $HOClH^+$ with our previous results for the isoelectronic HSOH shows some similarities but also some striking differences. $HOClH^+$ is predicted to have sufficient kinetic stability for a spectroscopic observation, as a barrier of more than 1 eV separates it from the more stable isomer H_2OCl^+. We also provide a summary comparing the whole series of axially chiral $HXYH^{(+)}$ isotopomers with X, Y = O, S, Se, Te, Cl and discuss the outlook for experiments on molecular parity violation in this series of molecular and ionic species. For the hydrogenic compounds D_2Te_2 is the only non-radioactive compound, in which parity violation is predicted to dominate over tunneling, similar to the chlorinated species Cl_2S_2, which we had investigated earlier.

Keywords: Stereomutation; $HOClH^+$; Reaction path Hamiltonian; Quasiadiabatic channels; H_2Te_2; Parity violation; Isotopes

1. Introduction

Mass spectrometry has a long history and high renown as an analytical technique and we may mention here some very practical applications [1,2]. However, mass spectrometry has also contributed to fundamental physics. We name as selected examples here the questions of the dynamics of electron impact ionization [3–5], studies in cluster physics [6–8], unimolecular fragmentation processes [9,10] or the proof of vibrational preionization of the very highly vibrationally excited neutral C_{60} after infrared multiphoton excitation [11]. In the present paper, we shall address the possibility of using transient species generated and observed in mass spectroscopy for the study of some fundamental dynamical aspects of chiral molecules relating to tunneling stereomutation and parity violation [12,13].

Parity violation in chiral molecules is known to lead to very small, but potentially observable effects [12–18] although so far no successful experiments have been reported [19]. In particular, if the barrier to stereomutation is large and thus hypothetical tunneling splittings for the symmetrical case are small, then, because of *de lege* asymmetry [12] one may observe a slight parity violating energy difference ΔE_{pv} between enantiomers, which corresponds to the reaction enthalpy $\Delta_{pv}H_0^\circ$ for the stereomutation reaction between enantiomers (similarly also P and M, see Fig. 1)

$$R \rightleftharpoons S \quad (1)$$

* Corresponding author. Tel.: +41-1-632-44-21; fax: +41-1-632-10-21
E-mail address: Martin@Quack.ch (M. Quack).
[1] Present address: Institute of Chemistry and Biotechnology (ICB), Zurich University of Applied Sciences (ZHW), Technikumstr. 9, CH-8401 Winterthur, Switzerland.

1387-3806/$ – see front matter © 2004 Elsevier B.V. All rights reserved.
doi:10.1016/j.ijms.2004.01.014

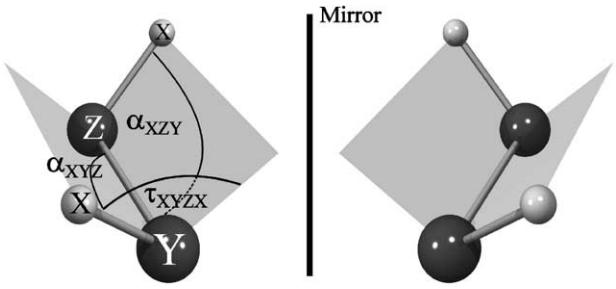

Fig. 1. Axially chiral structures and angle definitions of C_1-symmetric protonated hypochlorous acid $HOClH^+$ (Y = O, and Z = Cl) and C_2-symmetric hydrogen ditelluride H_2Te_2 (Y = Z = Te) isotopomers (X = H, D, and T) and their corresponding enantiomer, that is, mirror image molecule. Note that for H_2Te_2 the angle α_{XYZ} and α_{XZY} are identical. The left-hand side shows the P enantiomer, the right-hand side the M enantiomer.

$$\Delta_R H_0^\circ = \Delta_{pv} H_0^\circ = N_A \Delta E_{pv} \quad (2)$$

While this energy difference might be measured spectroscopically [20], it is expected to be very small, typically on the order of 10^{-12} J mol^{-1} or 10^{-17} eV [12]. The recent theoretical discovery that ΔE_{pv} is predicted to be one to two orders of magnitude larger [21–24] than anticipated from earlier calculations [18] has given new impetus to the field and the present work contributes to the new effort in this field [19–33].

From both an experimental and theoretical point of view, it would be of interest to study particularly simple prototype molecules or ions. Indeed, among the simplest chiral molecules are the axially chiral four-atomic molecules and ions of the type X–Y–Z–X$^{(+)}$ for which we show an example in Fig. 1, where Y and Z might also represent the same element.

The molecular and ionic systems we thus address in our study are the $HOClH^+$ ion and H_2Te_2 [34], of which the latter has been characterized in mass spectrometric experiments as a transient species. There have also been parity conserving quantum chemical studies of H_2Te_2 [35] and $HOClH^+$ [36–39]. This ion is isoelectronic to HSOH which has been generated in mass spectroscopic experiments [40] and more recently in bulk [41]. This molecule also falls in the general series of axially chiral molecules HXYH, for which we have already presented extensive calculations of parity violation and tunneling in our previous work [21–27,32,33,42,43]. However, it seems that, so far, parity violation has not been studied for an ionic species of this type. There is, however, interest in such a study because it has been suggested that ions could be more easily studied in traps than neutral molecules, in a spectroscopic search for molecular parity violation [44]. The disadvantages of such experiments on ions have been discussed as well, related to easy perturbation by weak electric fields that are best avoided [19,45]. Anticipating some of our results we note here that $HOClH^+$ itself turns out to be not very suitable for experiments on parity violation, because of the small magnitude of ΔE_{pv} compared to the tunneling splitting.

The situation for H_2Te_2 isotopomers turns out to be somewhat different because of larger ΔE_{pv} and smaller tunneling splittings. Its cathodic formation has been suggested in 1962 [46], more than 20 years later it has been synthesized by neutralization of ions in mass spectroscopy [34] and more recently it has been shown to be stable in the gas phase [47]. In H_2Te_2, because of the highly charged and neutron-rich nuclei, parity violation is expected to be much more important than in molecules involving lighter atoms [18–24]. Thus calculations ΔE_{pv} for H_2Te_2 have been carried out repeatedly before [48,49]. However, so far stereomutation tunneling has not been studied in this molecule. Therefore it was not known, whether H_2Te_2 would in fact be a good candidate for future experiments that aim to measure parity violating energy differences ΔE_{pv}, which is only possible if tunneling splittings $\Delta E_{\pm}$ are much smaller than ΔE_{pv}. We shall show in the present work that this is, indeed, the case for D_2Te_2 and T_2Te_2, of which the former should be rather easily accessible.

2. Theory and methods of calculation

2.1. Electronic structure calculations with parity conservation

The calculations of the electronic energy, forces, and force constants as needed for the reaction path calculations in Section 2.3 were done with the Gaussian 98 program package [50]. The electron correlation was included using the second-order Møller–Plesset perturbation theory (full MP2). For the choice of an appropriate basis set we performed for H_2Te_2 and for $HOClH^+$ several calculations using progressively larger basis sets. In the case of $HOClH^+$ the 6-31G, 6-311++G**, aug-cc-pVDZ and aug-cc-pVTZ standard all electron basis sets were used. For H_2Te_2 the following basis sets were used: (1, 2) the Los Alamos pseudopotentials LANL2DZ and LANL2DZDP (including polarization functions) [51] to describe the core region of the Te atom and a double zeta basis for its valence electrons and the all electron basis set aug-cc-pVDZ for the H atoms, and (3) the Stuttgart–Dresden–Bonn (sdb) relativistic effective core potential (see ref. [52]) with its corresponding basis sets (see ref. [53]), which are: (a) the sdb-cc-pVTZ and (b) the sdb-aug-cc-pVTZ (for Te) and in both cases the all electron basis set aug-cc-pVTZ for H, and (c) the sdb-aug-cc-pVQZ for Te and aug-cc-pVQZ for H. It is obvious that some of the above basis sets are really inadequate for our purposes, but they were used for comparison with earlier work, where available.

There are two isomers of the protonated hydrochlorous acid, $HOClH^+$ and H_2OCl^+. In the present work, the latter is calculated to be 5875.0 cm^{-1} more stable than $HOClH^+$ (this work, MP2/aug-cc-pVTZ). Our calculation is in good

agreement with a previous CCSD(T)/6-311++G**(3df,3pd) (using the CCSD(T)/6-311++G**(2df,2p) equilibrium structures) result of 5651.5 cm^{-1} [36]. To our knowledge there is no previous calculation for the barrier connecting these two isomers. We calculated a value of 9478.7 cm^{-1} for the electronic transition state energy with respect to the less stable isomer $HOClH^+$ (MP2/aug-cc-pVTZ; transition state structure: $r_{HCl} = 141.91$ pm, $r_{HO} = 98.89$ pm, $r_{ClO} = 177.28$ pm, $\alpha_{OClH} = 50.87°$, $\alpha_{ClOH} = 103.84°$, $\tau_{HClOH} = 103.49°$), which implies that $HOClH^+$ is a metastable isomer.

2.2. Calculation of parity violating potential energies

Under field free condition and upon neglecting nuclear spin interaction, the Hamiltonian which transforms odd under space inversion (or parity) is given by [22,24,31]

$$\hat{H}_{pv} \approx \frac{G_F}{2\sqrt{2}m_e c\hbar} \sum_a Q_W(a) \sum_i [\vec{s}_i \cdot \vec{p}_i, \delta^3(\vec{r}_i - \vec{r}_a)]_+ \quad (3)$$

with the Fermi coupling constant $G_F \approx 1.16639 \times 10^{-5}(\hbar c)^3$ (GeV)$^{-2} \approx 1.43586 \times 10^{-62}$ J m^3, the electron mass m_e, the velocity of light c, and Planck's constant $\hbar = h/2\pi$. $\vec{s}_i$ and $\vec{p}_i$ denote the electron spin and electron momentum operator, respectively, $[\ldots]_+$ is a shorthand notation for the anti commutator. In Eq. (3), summation is carried out over nuclei a and electrons i. The weak charge $Q_W(a)$ is

$$Q_W(a) \approx Z_a(1 - 4\sin^2\Theta_W) - N_A \quad (4)$$

where N_A denotes the neutron number, Z_a the nuclear charge and Θ_W the Weinberg angle with $\sin^2\Theta_W \approx 0.23117(16)$ [54].

Eq. (3) was used to determine the parity violating potential energy E_{pv} (Fig. 2). The reaction path – described in detail in the next section – calculated as a minimum energy path with the corresponding dihedral angle τ as leading coordinate (Fig. 1) provides a set of coordinates which have been used as input to our modification [24] of the DALTON program package [55] to determine E_{pv} within the multi-configurational linear response approach using RPA ("random phase approximation"), as described in detail elsewhere (see [24,56–58], and references cited therein).

We employed several basis sets to determine E_{pv} as a function of the reaction coordinate (corresponding approximately to the dihedral angle τ); there is no difference between the values obtained with RPA for the correlation consistent valence triple zeta bases (cc-pVTZ) and its augmented form (aug-cc-pVTZ), which is to be expected, and there is only a small deviation at the maxima and minima of the potential functions for the basis of double zeta quality (aug-cc-pVDZ). The transition state structures are planar with zero parity violating energy E_{pv} whereas the functional form of E_{pv} as function of the reaction coordinate is sinusoidal between consecutive transition state structures as found in all investigated parity violating potentials for torsional motion in H_2O_2 analogous compounds.

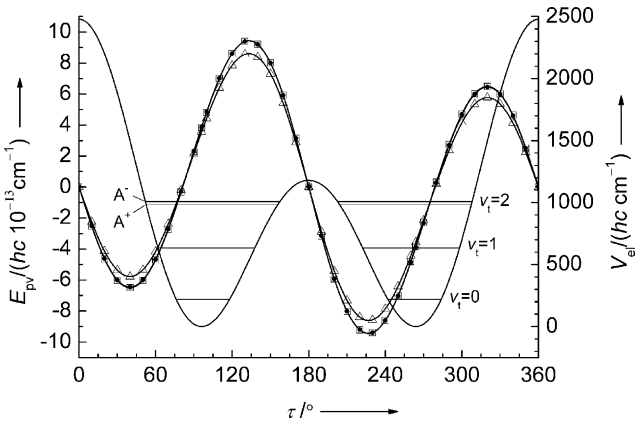

Fig. 2. Parity-conserving electronic torsional potential $V_{el}(\tau)$ (plain full line; MP2/aug-cc-pVTZ) and parity-violating potentials $E_{pv}(\tau)$ for $HOClH^+$ calculated employing RPA and different basis sets (full circles, aug-cc-pVTZ; squares, cc-pVTZ; triangles, aug-cc-pVDZ). Also shown are the torsional energy levels for different torsional states $\upsilon_t = 0$–2 of $HOClH^+$ that are superimposed on the electronic torsional potential. Only the torsional splitting $(\tilde{\nu}(A^-) - \tilde{\nu}(A^+))$ for the $\upsilon_t = 2$ level is large enough to be visible on this scale.

2.3. Reaction path hamiltonian calculation

In Fig. 1 the axially chiral structures and angle definitions of C_1-symmetric protonated hypochlorous acid $HOClH^+$ (Y = O and Z = Cl) and C_2-symmetric hydrogen ditelluride H_2Te_2 (Y = Z = Te) isotopomers (X = H, D, and T) and their corresponding enantiomer (mirror image molecule) are shown. In this figure we also included our angle definitions. For symmetry reasons we have for H_2Te_2: $\alpha_{XYZ} = \alpha_{XZY}$.

The torsional tunneling dynamics were calculated with the quasi-adiabatic channel-reaction path Hamiltonian (RPH) approach described in detail in [27,33,42,43]. Our treatment is a modified version of the RPH approach of Miller et al. [59] and is also conceptually related to the adiabatic channel model [60].

In this approach the complete vibrational Hamiltonian:

$$\hat{H}(\hat{p}, q, \{\hat{P}_k, Q_k\}) = \hat{H}_Q(\{\hat{P}_k, Q_k\}; q) + \hat{H}_q(\hat{p}, q) \quad (5)$$

is divided in two parts. The first part depends on the "fast" $3N - 7$ mass weighted normal coordinates Q_k and their conjugate momenta $\hat{P}_k$, and parametrically (indicated by the semicolon) upon the reaction coordinate q. The second part, which is the one dimensional Hamiltonian $\hat{H}_q(\hat{p}, q)$ depends only on the "slow" reaction coordinate q and its conjugate momentum $\hat{p}$ and is given by

$$\hat{H}_q = \tfrac{1}{2}\hat{p}G\hat{p} + u(q) + V_{el}(q) \quad (6)$$

with $u(q)$ as the pseudopotential (see [61]), V_{el} as the Born–Oppenheimer potential energy along the minimum energy path and G as the effective inverse reduced mass.

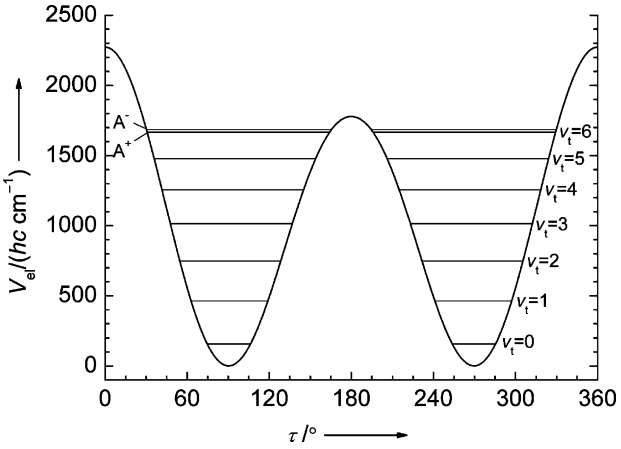

Fig. 3. Parity-conserving electronic torsional potential $V_{el}(\tau)$ of H_2Te_2 calculated employing MP2/sdb-aug-cc-pVTZ/aug-cc-pVTZ (Te/H) as well as torsional energy levels for different torsional states $v_t = 0$–6 of H_2Te_2 that are superimposed on the electronic torsional potential. Only the torsional splitting $(\tilde{\nu}(A^-) - \tilde{\nu}(A^+))$ for the $v_t = 6$ level is large enough to be visible on this scale.

For the full Hamiltonian $\hat{H}$ the eigenfunctions are approximated as follows:

$$\Psi_m^{(n)}(\vec{Q}, q) = \chi_m^{(n)}(q)\varphi_n(\vec{Q}; q) \quad (7)$$

$$(\langle\varphi_n|\hat{H}|\varphi_n\rangle_Q - E_m^{(n)})\chi_m^{(n)}(q) = 0 \quad (8)$$

where $\varphi_n(\vec{Q}; q)$ represents the eigenfunctions of the Hamiltonian (Eq. (5)) at fixed values of q. We approximated these eigenfunctions by a product of one-dimensional harmonic oscillator functions $\psi_{n_k}^{(k)}(Q_k; q)$ so that n becomes a multi-index:

$$\varphi_n(\vec{Q}; q) = \prod_{k=1}^{3N-7} \psi_{n_k}^{(k)}(Q_k; q) \quad (9)$$

The potential energy along the reaction path calculated as a minimum energy path is shown in Fig. 2 for $HOClH^+$ and in Fig. 3 for H_2Te_2. We calculated the minimum energy path as follows: for a given fixed dihedral angle τ we optimize, with respect to minimal electronic potential energy, all the remaining degrees of freedom ("clamped coordinate" approach). This minimum energy path has the advantage that it is invariant under isotopic substitution. For H_2Te_2 as well as for $HOClH^+$ the corresponding dihedral angles τ were chosen as leading coordinate represented in Fig. 1. The path itself was calculated in steps of 10° and an interpolation in the path length coordinate q employing the calculated points, led to a path consisting of 179 grid points. Finally, Eq. (8) was solved numerically in a discrete variable representation [43,62]. We used a 128-bit word length (quadruple precision) for a floating-point number and fitted the effective potentials, all harmonic transition wavenumbers $(\tilde{\omega}_i(q))$ and the effective inverse reduced masses as functions of the reaction coordinate with Fourier series, which acted as filters for the numerical noise. This procedure, described in detail in ref. [25], enables us to numerically "resolve" even tunneling splittings of about 10^{-28} cm^{-1} (see ref. [26]).

3. Results and discussion

3.1. $HOClH^+$ $DClOD^+$ and $TClOT^+$

The fundamentals of $HOClH^+$ have to our knowledge not been observed, so far. However, there is one extensive previous theoretical study [36] in which the harmonic wavenumbers and the equilibrium structure for various basis sets were calculated at the MP2 and at the CCSD(T) level of theory. (CCSD(T) stands for coupled-cluster theory including single and double excitations explicitly and triple excitations with a perturbative approach). Table 1 presents our predictions for the harmonic wavenumbers and Table 2 shows the optimized equilibrium structures as well as the calculated *cis* and *trans* barrier heights, $V_{el,trans}$ and $V_{el,cis}$ (with $V_{el,trans} = V(\tau = 180°) - V(\tau_{min})$ and $V_{el,cis} = V(\tau = 0°) - V(\tau_{min})$), of the torsional electronic potential energy for four different basis sets (as described above) on the MP2 level of theory and also the results of CCSD(T) calculations with a 6-31G$^+$ and a 6-31G(2df,2p) (only in Table 2) basis sets [36].

The results for all basis sets agree for the four largest harmonic vibrations within a few percent. For ω_5 (the Cl–O stretching vibration) and for ω_6 (the torsional motion) large deviations up to about 20% are present when comparing the MP2/aug-cc-pVTZ and the corresponding CCSD(T)/6-31G* calculation. The CCSD(T) level of theory may be considered to be, in principle, superior to the MP2 level of theory, but the 6-31G* basis set used in the CCSD(T) calculation is rather small and therefore it is

Table 1
Calculated harmonic wavenumbers ω_i of $HClOH^+$ at the MP2 level of theory (if not otherwise quoted) for various basis sets

	6-31G*	6-311++G**	aug-cc-pVDZ	aug-cc-pVTZ	CCSD(T) (6-31G*) [36]
ω_1	3564.2	3690.0	3591.5	3615.3	3562.0
ω_2	2807.1	2811.5	2731.5	2742.6	2754.0
ω_3	1388.9	1294.0	1342.6	1346.1	1378.0
ω_4	1009.1	1011.6	977.5	1014.9	974.0
ω_5	767.0	736.6	762.2	790.8	680.0
ω_6	443.5	412.6	443.3	460.4	424.0

All values are given in cm^{-1}. In the following assignments 's' refers to a stretching and 'b' to a bending mode: ν_1 = s-(HO), ν_2 = s-(HCl), ν_3 = b-(HOCl), ν_4 = b-(HClO), ν_5 = s-(ClO) and ν_6 = torsion.

Table 2
Calculated optimized *cis* and *trans* saddle point energies (electronic potential energy: $V_{el,trans} = V_{el}(\tau = 180^\circ) - V_{el}(\tau(HClOH^+, \text{min. geo.}))$ and $V_{el,cis} = V_{el}(\tau = 0^\circ) - V_{el}(\tau(HClOH^+, \text{min. geo.}))$) and calculated equilibrium geometries of $HClOH^+$ for various basis sets on the MP2 level of theory (if not otherwise noted)

	r_{HO} (pm)	r_{ClO} (pm)	r_{HCl} (pm)	α_{HOCl} (°)	α_{HClO} (°)	τ_{HClOH} (°)	$V_{el,trans}$ (cm^{-1})	$V_{el,cis}$ (cm^{-1})
6-311++G**	97.8	166.4	130.5	105.7	98.8	100.5	860.3	2624.6
aug-cc-pVDZ	98.7	167.9	132.2	104.8	98.6	97.5	1057.5	2438.0
aug-cc-pVTZ	98.1	163.8	130.9	105.8	99.7	96.0	1181.6	2480.3
CCSD(T) (6-31G+) [36]	99.1	168.0	131.0	105.9	98.9	100.4	–	–
CCSD(T) (6-31G(2df,2p)) [36]	97.7	165.3	131.1	105.1	99.7	96.3	–	–
Trans-TS (aug-cc-pVTZ)	98.1	166.3	130.6	93.5	104.4	180.0	–	–
Cis-TS (aug-cc-pVTZ)	98.1	165.8	130.6	103.5	108.1	0.0	–	–

For comparison results of previous work are also shown as well as the transition states (TS) at the aug-cc-pVTZ level of theory.

Table 3
Harmonic wavenumbers ω_i calculated ab initio for $XClOX^+$ (X = H, D, T) with the aug-cc-pVTZ basis set on the MP2-level of theory

	ω_1	ω_2	ω_3	ω_4	ω_5	ω_6
$HClOH^+$	3615.3	2742.6	1346.1	1014.9	790.8	460.4
$DClOD^+$	2634.3	1968.1	983.9	721.5	807.6	337.3
$TClOT^+$	2214.9	1630.9	838.4	613.9	784.6	283.6

The ω_i are given in cm^{-1}. The numbering of the fundamentals of $DClOD^+$ and $TClOT^+$ corresponds to the $HClOH^+$ fundamentals (see Table 1 for descriptions).

anticipated that the results are not converged with respect to the basis set size. This is further confirmed by a comparison of the equilibrium structures (Table 2) where large deviations between the results of a CCSD(T)/6-31G* calculation and a CCSD(T)/6-31G(2df,2p) calculation (with only a somewhat larger basis set) are observed, whereas an excellent agreement was found between the latter and the MP2/aug-cc-pVTZ results. Therefore we decided to use the aug-cc-pVTZ basis set on the MP2 level of theory in our calculations as the best compromise between accuracy and computational cost for the complete reaction path calculation. Fig. 2 shows the potential energy function for the reaction path. Overall, the behavior is very similar to the isoelectronic neutral species HSOH but the difference between *cis* and *trans* barrier heights is larger in $HOClH^+$ than in HSOH.

In Table 3 we summarize all calculated ab initio (MP2/sdb-aug-cc-pVTZ) harmonic wavenumbers for $HClOH^+$, $DClOD^+$ and $TClOT^+$. The numbering of the fundamentals corresponds to the $HClOH^+$ isotopomer convention.

Table 4 summarizes the results for the torsional tunneling splittings

$$\Delta\tilde{\nu}_t = \tilde{\nu}(A^-) - \tilde{\nu}(A^+) \quad (10)$$

of the first six pure torsional states and the torsional wavenumbers $\tilde{\nu}(A^+)$ with respect to the corresponding zero point level of $HOClH^+$ and its fully deuterated and tritiated isotopomers for calculations on the MP2 level of theory with the aug-cc-pVTZ basis sets. As mentioned above no experimental tunneling splittings are known for these molecules. We expect that our data are good estimates for these small tunneling splittings and might be useful as guidance for future experimental work. Our results indicate that all tunneling splittings should be experimentally accessible with high resolution spectroscopy. The accuracy of the RPH approach itself was discussed in detail previously [25,43]. We have also shown recently that with appropriate empirical corrections the modest intrinsic ab initio error in the electronic structure calculations can be further reduced [63]. Fig. 2 shows the lowest six torsional levels (υ_t = 0–2) in their position related to the potential.

Table 4
Torsional tunneling splittings $\Delta\tilde{\nu}_t = \tilde{\nu}(A^-) - \tilde{\nu}(A^+)$ for pure torsional states $|\upsilon_t\rangle$, where υ_t is the torsional quantum number in high barrier notation, and the corresponding $\tilde{\nu}(A^+)$ (with respect to the corresponding zero point level, whose wavenumber is given in the column "0") of $XClOX^+$ with X = H, D or T calculated within our quasi-harmonic quasi-adiabatic channel RPH approximation (MP2/aug-cc-pVTZ)

	$\Delta\tilde{\nu}_t$					
υ_t	0	1	2	3	4	5
$HClOH^+$	1.63×10^{-2}	1.02	22.5	117.74	181.96	199.86
$HClOD^+$	1.67×10^{-4}	1.58×10^{-2}	0.62	12.06	72.62	124.27
$TClOT^+$	6.69×10^{-6}	7.84×10^{-4}	4.02×10^{-2}	1.14	16.71	71.90
	$\tilde{\nu}(A^+)$					
$HClOH^+$	4972.81	415.99	767.55	1021.03	1323.15	1693.03
$DClOD^+$	3724.20	314.24	603.20	853.62	1037.46	1240.32
$TClOT^+$	3181.51	267.57	518.24	748.21	942.42	1087.71

All values are given in cm^{-1}.

Table 5
Mode specific stereomutation tunneling of $XClOX^+$ (X = H, D, or T): torsional tunneling splittings $\Delta\tilde{\nu}_i = \tilde{\nu}(A^-) - \tilde{\nu}(A^+)$ for the excitation of a fundamental ν_i (RPH with MP2/aug-cc-pVTZ)

		ν_0	ν_1	ν_2	ν_3	ν_4	ν_5	ν_6
$HClOH^+$	$\Delta\tilde{\nu}_i$ ($\times 10^{-2}$ cm^{-1})	1.62	1.64	1.34	1.44	1.86	1.74	102
$DClOD^+$	$\Delta\tilde{\nu}_i$ ($\times 10^{-4}$ cm^{-1})	1.67	1.68	1.38	1.44	1.92	1.93	158
$TClOT^+$	$\Delta\tilde{\nu}_i$ ($\times 10^{-6}$ cm^{-1})	6.69	6.68	5.51	6.07	8.15	7.34	784

In previous work we have demonstrated by comparison with experimental results that for the rather similar examples H_2O_2 [43] and H_2S_2 [25] the stereomutation tunneling is well approximated by the present approach. Moreover for H_2O_2, a direct validation was possible by comparison with a fully six-dimensional, "exact" DVR and a full dimensional Quantum Monte Carlo calculation [43,62,64], as a complete six-dimensional potential hypersurface is available [64]. The approximate and exact tunneling splittings are generally almost identical except in the cases of excited states with local resonances. From past experience we expect the torsional tunneling splittings to be rather accurate, whereas the absolute energy of the zero point level is only a rough approximation.

As expected the data in Table 4 indicate that an isotopomer with a higher effective reduced tunneling mass has a smaller tunneling splitting and a correspondingly longer tunneling time. We predict here an increase of more than three orders of magnitude for the stereomutation time $t_s = (2c\Delta\tilde{\nu}_t)^{-1}$ in going from $HOClH^+$ ($t_s = 1.0 \times 10^{-9}$ s) to $TClOT^+$ ($t_s = 2.5 \times 10^{-6}$ s) (ground state values). This behavior is similar to what has been observed for HOOH, HSSH, and HSOH, but not as pronounced as in H_2Se_2 [33] or H_2Te_2 (see next section).

In chemical reaction dynamics a current question concerns vibrational mode selectivity [65–68]. As we have discussed for the case of H_2O_2 [43], H_2S_2 [25], Cl_2S_2 [26], and hydrogenthioperoxide isotopomers [27] it is of interest whether certain non-torsional vibrational modes promote ("catalyze") or inhibit the stereomutation dynamics. The results of our investigation of the mode selectivity of the tunneling process in $HOClH^+$ (and the corresponding D and T isotopomers) are summarized in Table 5 and compared to our previous work on HSOH analogous molecules in Fig. 4. In this figure we show the relative deviations $\Delta\Delta\tilde{\nu}_i/\Delta\tilde{\nu}_0$ (with $\Delta\Delta\tilde{\nu}_i = \Delta\tilde{\nu}_i - \Delta\tilde{\nu}_0$) from the ground state torsional tunneling splittings $\Delta\tilde{\nu}_0$ due to excitation of non-torsional fundamentals for XYOX dichalcogenide molecules with X = H, D, T and Y = Cl, S (Z = Oxygen).

The excitation of a XY stretching or a XOY bending fundamental leads for all molecules to an inhibition of the stereomutation tunneling dynamics, corresponding to a decrease of the tunneling splittings by about 20%. A rather small influence on the stereomutation dynamics has the excitation of the XO stretching mode. The YO stretching fundamental appears also to be an inactive mode or a weak promoting mode. However, the XYO bending vibrational mode is a relative strong promoting mode (about 30%). There is a general trend visible in this figure that the changes of tunneling splittings upon various vibrational excitations are larger for HSOH than for the ionic $HOClH^+$.

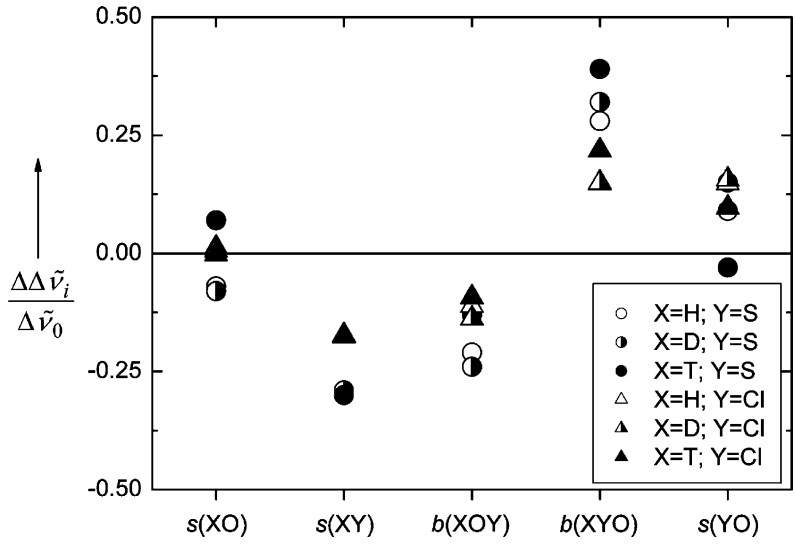

Fig. 4. Relative deviations $\Delta\Delta\tilde{\nu}_i/\Delta\tilde{\nu}_0$ (with $\Delta\Delta\tilde{\nu}_i = \Delta\tilde{\nu}_i - \Delta\tilde{\nu}_0$) from the ground state torsional tunneling splittings $\Delta\tilde{\nu}_0$ due to excitation of non-torsional fundamentals for XYZX dichalcogenides molecules and cations with X = H, D, T and Y = S (i.e., hydrogen thioperoxide) and Y = Cl (i.e., protonated hypochlorous acid). The data for Y = S are from ref. [27] (Z = Oxygen).

Table 6
Calculated harmonic wavenumbers ω_i for H_2Te_2 (at the MP2 level of theory with various basis sets which are given for the Te atom)

	LANL2DZ	LANL2DZDP	sdb-cc-pVTZ	sdb-aug-cc-pVTZ	sdb-aug-cc-pVQZ
ω_1	2237.1	2187.3	2195.8	2191.7	2210.72
ω_2	563.9	613.8	621.7	618.43	622.35
ω_3	305.8	315.79	329.3	323.9	330.92
ω_4	170.8	201.32	211.9	209.9	213.18
ω_5	2237.9	2187.6	2196.2	2193.2	2212.42
ω_6	565.6	614.7	625.2	618.5	622.45

For the H atoms the aug-cc-pVDZ (in combination with LANL2DZ and LANL2DZDP for Te), the aug-cc-pVTZ (in combination with sdb-cc-pVTZ and sdb-aug-cc-pVTZ for Te) and aug-cc-pVQZ (in combination with sdb-aug-cc-pVQZ for Te) are employed. All values are given in cm^{-1}. In the following assignments 's' refers to a stretching and 'b' to a bending mode: ν_1 = sym.-s(HTe), ν_2 = sym.-b(HTeTe), ν_3 = torsion, ν_4 = s(TeTe), ν_5 = asym.-s(HTe) and ν_6 = asym.-b(HTeTe).

Finally, we compare the tunneling splittings with the parity-violating energy difference ΔE_{pv}. The parity violating potential as a function of the torsional angle τ is shown in Fig. 2. There is a modest basis set dependence when going from aug-cc-pVDZ to aug-cc-pVTZ. We notice that the general form of this function and also the maximum of the absolute value (about $10 \times 10^{-13}\,cm^{-1}$ for $\tau \approx 130^\circ$) of the parity violating potential is almost identical with the corresponding results for HSOH (maximum of about $10 \times 10^{-13}\,cm^{-1}$ for $\tau \approx 135^\circ$). In principle one would expect this similarity, because of the similar electroweak charge of the Cl atom compared with that of the S atom and the fairly similar, isoelectronic structure. We define an electronic parity-violating energy difference between the two enantiomers at their equilibrium structures as the difference ΔE_{pv}^{el} of the parity-violating potentials at the dihedral angle $\tau = 96$ and 276° for the P und M enantiomers.

$$\Delta E_{pv}^{el} \approx E_{pv}(P; 96^\circ) - E_{pv}(M; 276^\circ) \quad (11)$$

$$\Delta E_{pv}^{el} \approx 2E_{pv}(P; 96^\circ) \simeq (hc)7.74 \times 10^{-13}\,(cm^{-1}) \quad (12)$$

This result is almost isotopomer independent. Thus the comparison with the isotopomer dependent tunneling splittings in Table 4 indicates that tunneling dominates by far over parity violation for all three isotopomers and thus there is actually no observable parity violating ground state energy difference for the enantiomers [12].

3.2. H_2Te_2 and its isotopomers

For H_2Te_2 there are to our knowledge neither experiments nor previous calculations for its six fundamental vibrations. Table 6 compares the harmonic wavenumbers that were calculated ab initio on the MP2 level of theory as described in Section 2.1 with five different basis sets. Taking the largest basis set as reference the results for the four largest basis sets agree for all harmonic wavenumbers within a few percent. The smallest, which is the LANL2DZ basis set, shows deviations up to about 20%. Similar to the calculation for H_2Se_2 [33] we consider the latter basis to be unreliable.

In Table 7 the optimized equilibrium structures as well as the calculated *cis* and *trans* barrier heights and transition state structures, $V_{el,trans}$ and $V_{el,cis}$, are listed and compared with results of previous theoretical work, where available. The results presented in Tables 6 and 7 indicate that the Stuttgart quasi-relativistic pseudo-potentials with

Table 7
Calculated optimized *cis* and *trans* saddle point energies (electronic potential energy: $V_{el,trans} = V_{el}(\tau = 180^\circ) - V_{el}(\tau(H_2Te_2, \text{min. geo.}))$ and $V_{el,cis} = V_{el}(\tau = 0^\circ) - V_{el}(\tau(H_2Te_2, \text{min. geo.}))$ and calculated equilibrium geometries of H_2Te_2 for various basis sets on the MP2 level of theory (if not otherwise noted)

	r_{TeTe} (pm)	r_{HTe} (pm)	α_{HTeTe} (°)	τ_{HTeTeH} (°)	$V_{el,trans}$ (cm^{-1})	$V_{el,cis}$ (cm^{-1})
MP2/sdb-aug-cc-pVQZ	267.6	164.8	95.38	90.31	1830.9	2348.0
MP2/sdb-aug-cc-pVTZ	269.1	165.29	95.30	90.20	1780.8	2276.5
MP2/sdb-cc-pVTZ	269.29	165.26	95.27	89.61	1821.3	2044.21
MP2/LANL2DZDP	272.55	165.37	94.24	90.17	1655.4	2124.5
MP2/LANL2DZ	284.16	162.80	91.80	89.38	1483.9	1919.0
MBPT2[a] [49]	284.0	164.0	94–96[b]	–	–	–
SCF/min. Slater basis [72]	272.7	167.7	92.47	90.0	1262.0	1471.0
SCF/MINI-1* [73]	293.3	165.5[c]	90.6[c]	90.3	–	–
EPT[d] [74]	–	–	–	–	1469.0	1259.0
Trans-TS (sdb-aug-cc-pVTZ)	269.3	165.3	95.27	180.0	–	–
Cis-TS (sdb-aug-cc-pVTZ)	275.4	164.8	91.48	0.0	–	–

For comparison results of previous work are also shown as well as the transition states (TS) at the aug-cc-pVTZ level of theory.
[a] MBPT2 stands for "second-order many-body perturbation theory" (see ref. [49], also for basis set details).
[b] Range for which α is expected for H_2S_2, H_2Se_2 and H_2Te_2.
[c] Kept fixed during geometry optimization.
[d] EPT stands for "exchange perturbation theory".

Table 8
Harmonic wavenumbers ω_i calculated ab initio and band strengths G_i of X_2Te_2 (X = H, D, T) calculated with the sdb-aug-cc-pVTZ/aug-cc-pVTZ (Te/H) basis set on the MP2-level of theory in the double harmonic approximation

	ω_1	ω_2	ω_3	ω_4	ω_5	ω_6
H_2Te_2	2191.7	618.4	323.9	209.9	2193.2	618.5
D_2Te_2	1556.4	438.9	230.2	209.8	1557.4	440.6
T_2Te_2	1276.9	359.9	188.7	210.1	1277.8	362.5
	G_1	G_2	G_3	G_4	G_5	G_6
H_2Te_2	0.175	0.0002	0.005	0.001	0.235	0.919
D_2Te_2	0.124	1.1×10^{-4}	0.003	0.001	0.166	0.656
T_2Te_2	0.101	9.0×10^{-5}	0.003	0.0007	0.135	0.541

The ω_i are given in cm^{-1} and the G_i in pm^2. The numbering of the fundamentals of T_2Te_2 corresponds to the H_2Te_2 or D_2Te_2 fundamentals.

their corresponding basis sets of triple zeta or quadruple zeta quality at the MP2 level of theory should be adequate for our investigation. It is obvious that the changes in the results for the LANL2DZDP basis set compared with those of the LANL2DZ basis set are pointing in the direction of the results of the larger basis sets. As we aim at a well balanced overall description under the consideration of the computational costs we decided to use in general the sdb-aug-cc-pVTZ basis set in our investigation. Fig. 3 shows the torsional potential and the corresponding torsional levels calculated in the RPH approximation. In Table 8 we list all calculated ab initio harmonic wavenumbers for H_2Te_2, D_2Te_2 and T_2Te_2 as well as the corresponding band strengths in terms of the integrated cross sections G_i. The values for G_i are calculated in the double harmonic approximation and are defined through the practical Eq. (13) [69]:

$$G_i = \frac{8\pi^3}{(4\pi\epsilon_o)(3hc)}|\langle v_i = 1|\mu|v_i = 0\rangle|^2 \cong 41.624\left(\frac{|\langle v_i = 1|\mu|v_i = 0\rangle|}{\text{Debye}}\right)^2 (\text{pm}^2) \quad (13)$$

where μ is the electric dipole moment operator. Reporting G_i has the advantage in contrast to the frequently reported $A_i = \omega_i \times N_A \times G_i$ that no additional error is introduced in G_i through the usually large ab initio error in the harmonic wavenumbers ω_i.

Table 9 shows the tunneling splittings for the first six pure torsional levels and also the positions of the lower tunneling levels $\tilde{\nu}(A^+)$ with respect to the corresponding zero point level of H_2Te_2 and its fully deuterated and tritiated isotopomers. The torsional tunneling splittings calculated with the LANL2DZDP basis set are also given in order to get a conservative estimate of the uncertainties in our ab initio predictions. Overall we find, as expected from the above discussion, a basis set dependence for the values of the torsional tunneling splittings and the corresponding levels with a maximum variation of the tunneling splittings for T_2Te_2 in the range of a factor of 10 (for the vibrational ground state). For the other isotopomers and/or higher torsional excitations these deviations decrease to a factor of about 2. The tunneling splittings calculated with the LANL2DZDP basis set are in any case larger, which is expected, because the *trans* barrier height $V_{el,trans}$ is about 180 cm^{-1} lower than those of the larger basis sets, which should be much more reliable (see above). However, even such large differences have no influence on the conclusions to be drawn below on the importance of parity violation in various hydrogen ditelluride isotopomers.

Normally, an isotopomer with a higher effective reduced tunneling mass has a longer tunneling time. For the stereomutation time ($t_s = (2c\Delta\tilde{\nu}_t)^{-1}$) an increase of about eight orders of magnitude is predicted for the vibrational ground state in going from H_2Te_2 ($t_s = 6 \times 10^{-4}$ s) to T_2Te_2 ($t_s =$ 66138 s). All molecules of the type XYZX investigated up to now show such a behavior but the effects are most pronounced for the H_2Te_2 isotopomers.

We expect that our data, especially for the calculations with the sdb-aug-cc-pVTZ basis sets, are good estimates to within an uncertainty of less than a factor of 2–10 for these very small tunneling splittings. They might be used as a guide in future ro-vibrational experimental investigations.

The torsional mode ω_3 (e.g., Table 6) is not the lowest in frequency for H_2Te_2 and its isotopomers but rather the (Te–Te)-stretching mode ω_4 is lowest. This raises the question whether the adiabatic separation of the torsional mode from the other modes is adequate here. However, it has been found that this separation may be adequate, even if the torsional mode is not the lowest, and even for highly excited states (see e.g., [63]). Thus we do not expect our conclusions to be affected by this approximation except for local resonances, as usual. Also, a two-dimensional treatment of tunneling including the lowest two modes could be used to check this assumption. However, any error introduced by this is expected to be smaller than the errors from the potential energy calculations.

We have also investigated the vibrational mode selectivity of the stereomutation dynamics and the results are listed in Table 10 together with our previous work on the whole series of dihydrogen-dichalocogenides in Fig. 5 where the relative

Table 9
Torsional tunneling splittings $\Delta\tilde{\nu}_t = \tilde{\nu}(A^-) - \tilde{\nu}(A^+)$ for pure torsional levels $|v_t\rangle$ (with the torsional quantum number v_t in the high barrier notation) and the corresponding $\tilde{\nu}(A^+)$ (with respect to the corresponding zero point level, whose wavenumber is given in the column "0") of X_2Te_2 with X = H, D or T calculated within our quasi-harmonic quasi-adiabatic channel RPH approximation (MP2/sdb-aug-cc-pVTZ/aug-cc-pVTZ (Te/H) and MP2/LAN2DZDP/aug-cc-pVDZ (Te/H))

	$\Delta\tilde{\nu}_t$					
v_t	0	1	2	3	4	5
MP2/sdb-aug-cc-pVTZ						
H_2Te_2	2.75×10^{-8}	3.79×10^{-6}	2.24×10^{-4}	7.56×10^{-3}	0.16	2.31
D_2Te_2	1.17×10^{-12}	2.20×10^{-10}	1.91×10^{-8}	1.02×10^{-6}	3.75×10^{-5}	1.00×10^{-3}
T_2Te_2	2.52×10^{-16}	1.32×10^{-13}	1.42×10^{-11}	9.54×10^{-10}	4.53×10^{-8}	1.61×10^{-6}
	$\tilde{\nu}(A^+)$					
H_2Te_2	3074.37	306.54	591.58	856.25	1100.60	1322.29
D_2Te_2	2214.59	221.90	434.47	637.69	831.44	1015.44
T_2Te_2	1836.21	183.44	360.97	532.51	697.95	857.12
LAN2DZDP						
H_2Te_2	6.21×10^{-8}	8.65×10^{-6}	5.01×10^{-4}	1.64×10^{-2}	0.33	4.39
D_2Te_2	3.69×10^{-12}	7.04×10^{-10}	6.12×10^{-8}	3.22×10^{-6}	1.15×10^{-4}	2.97×10^{-3}
T_2Te_2	2.35×10^{-15}	5.42×10^{-13}	5.85×10^{-11}	3.93×10^{-9}	1.84×10^{-7}	6.39×10^{-6}
	$\tilde{\nu}(A^+)$					
H_2Te_2	3056.18	297.85	572.45	826.06	1058.81	1267.02
D_2Te_2	2200.47	216.01	421.91	617.97	804.19	980.30
T_2Te_2	1823.86	178.70	350.99	516.92	676.46	829.48

All values are given in cm^{-1}.

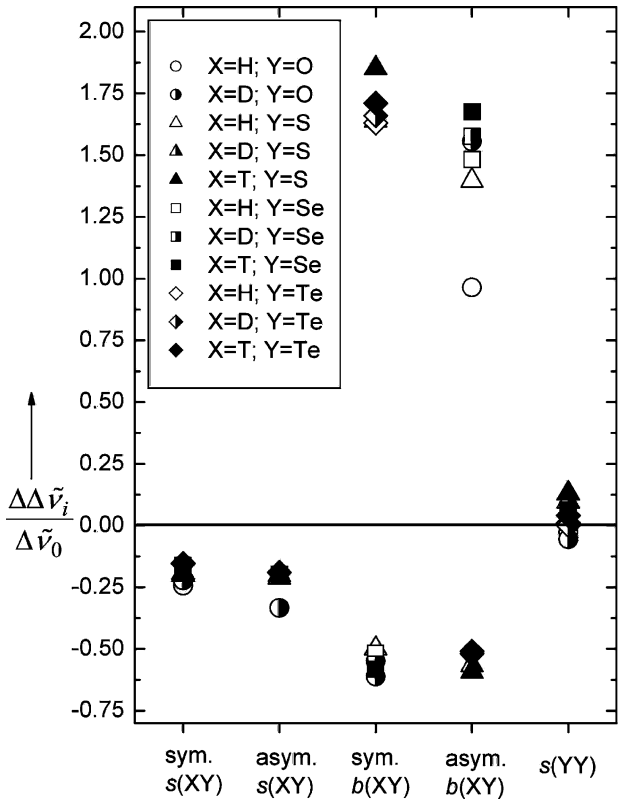

Fig. 5. Relative deviations $\Delta\Delta\tilde{\nu}_i/\Delta\tilde{\nu}_0$ (with $\Delta\Delta\tilde{\nu}_i = \Delta\tilde{\nu}_i - \Delta\tilde{\nu}_0$) from the ground state torsional tunneling splittings $\Delta\tilde{\nu}_0$ due to excitation of non-torsional fundamentals for X_2Y_2 dichalcogenides molecules with X = H, D, T and Y = O, S, Se, Te. The data for Y = O are from ref. [43], the one for Y = S from ref. [25], and the data for Y = Se from ref. [33].

deviations $\Delta\Delta\tilde{\nu}_i/\Delta\tilde{\nu}_0$ (with $\Delta\Delta\tilde{\nu}_i = \Delta\tilde{\nu}_i - \Delta\tilde{\nu}_0$) from the ground state torsional tunneling splittings $\Delta\tilde{\nu}_0$ due to excitation of non-torsional fundamentals for X_2Y_2 dichalcogenide molecules with X = H, D, T and Y = O, S, Se and Te are shown.

For all molecules investigated an excitation of a XY stretching fundamental leads to an inhibition of the stereomutation tunneling dynamics, corresponding to a decrease of the tunneling splittings by about 20%. This behavior is similar to that for XSOX and $XClOX^+$ (see Fig. 4) with the exception for Y = O, where for the two latter molecules the XO stretching mode is rather ineffective. The YY stretching fundamental appears on the average as inactive mode for the process of stereomutation. The XYY bending vibrational modes are either strongly promoting (about 100–200%) or inhibiting (about 60%). The corresponding values for XSOX and $XClOX^+$ (Fig. 3) are in accordance with these observations but the effects are smaller by a factor of more than 2.

Overall it is of interest that the relative effects are so similar, while the absolute values for the corresponding tunneling splittings differ over 17 orders of magnitude.

Finally, we compare the tunneling splittings with the parity-violating energy difference ΔE_{pv}^{el}. In Table 11 we summarize results for the current best estimates of $|\Delta E_{pv}^{el}|$ and $\Delta E_{\pm}$ (rounded values for the vibrational ground state) for a series of dichalcogenides XYZX. Because of the low electroweak charges of the hydrogen isotope nuclei the parity-violating energy differences for the isotopomers can be assumed to be similar.

Table 10
Mode specific stereomutation tunneling of X_2Te_2 (X = H, D, or T): torsional tunneling splittings $\Delta\tilde{\nu}_i = \tilde{\nu}(A^-) - \tilde{\nu}(A^+)$ for the excitation of a fundamental ν_i (RPH with MP2/sdb-aug-cc-pVTZ/aug-cc-pVTZ (Te/H) data)

		ν_0	ν_1	ν_2	ν_3	ν_4	ν_5	ν_6
H_2Te_2	$\Delta\tilde{\nu}_i/(10^{-8}\,cm^{-1})$	2.74	2.32	7.21	379	2.76	2.22	1.42
D_2Te_2	$\Delta\tilde{\nu}_i/(10^{-12}\,cm^{-1})$	1.17	0.99	3.11	220	1.17	0.95	0.57
T_2Te_2	$\Delta\tilde{\nu}_i/(10^{-16}\,cm^{-1})$	5.80	4.90	15.72	1320	6.03	4.70	2.76

Table 11
Theoretically calculated $|\Delta E_{pv}^{el}|$ and $\Delta E_{\pm}$ for various molecules

Molecule	$\lvert\Delta E_{pv}^{el}\rvert$ (cm^{-1})	$\Delta E_{\pm}$ (cm^{-1})	Reference
H_2O_2	4×10^{-14}	11	[24,43,75]
D_2O_2	4×10^{-14}	2	[24,43]
T_2O_2	4×10^{-14}	0.5	[27]
HSOH	4×10^{-13}	2×10^{-3}	[27]
DSOD	4×10^{-13}	1×10^{-5}	[27]
TSOT	4×10^{-13}	3×10^{-7}	[27]
$HClOH^+$	8×10^{-13}	2×10^{-2}	This work
$DClOD^+$	–[c]	2×10^{-4}	This work
$TClOT^+$	–[c]	7×10^{-6}	This work
H_2S_2	1×10^{-12}	2×10^{-6}	[25]
D_2S_2	1×10^{-12}	5×10^{-10}	[25]
T_2S_2	1×10^{-12}	1×10^{-12}	[25]
Cl_2S_2	1×10^{-12}	$\approx 10^{-76}$ [a]	[26]
H_2Se_2	2×10^{-10} [49][d]	1×10^{-6}	[33]
D_2Se_2	–[c]	3×10^{-10}	[33]
T_2Se_2	–[c]	4×10^{-13}	[33]
H_2Te_2	3×10^{-9} [49][b]	3×10^{-8}	This work
D_2Te_2	–[c]	1×10^{-12}	This work
T_2Te_2	–[c]	3×10^{-16}	This work

Values for ΔE_{pv}^{el} are calculated at the equilibrium structures without vibrational corrections if not otherwise indicated.

[a] Extrapolated value.

[b] Calculated for the *P*-structure (r_{TeTe} = 284 pm, r_{HTe} = 164 pm, α_{HTeTe} = 92° and τ_{HTeTeH} = 90°) and the corresponding *M*-structure. An earlier, very approximate result by Wiesenfeld [48] may be quoted as well, giving $\Delta E_{pv} = 8 \times 10^{-10}\,cm^{-1}$ for the following structure: r_{TeTe} = 271.2 pm, r_{HTe} = 165.8 pm, α_{HTeTe} = 90° and τ_{HTeTeH} = 90°).

[c] Expected to be very similar to the corresponding hydrogen isotopomers.

[d] Calculated for the *P*-structure (r_{HSe} = 145 pm, α_{HSeSe} = 92° and τ_{HSeSeH} = 90°) and the corresponding *M*-structure.

4. Conclusions and outlook

The combination of appropriate ab initio calculations and the quasi-adiabatic channel quasi-harmonic reaction path Hamiltonian approach [43] is suitable to make quantitative, ab initio predictions for the stereomutation tunneling splittings.

We have previously demonstrated excellent agreement with the available experimental data from H_2O_2, HSOH, H_2S_2 and CH_3OH. Here we present for H_2Te_2 and $HClOH^+$ and their hydrogen isotopomers the theoretical predictions for the torsional tunneling splittings in the levels with v_t = 0–5. While refined calculations, including relativistic effects in more detail, are desirable particularly for H_2Te_2, the main conclusions that we can draw here concerning several important questions should be insensitive to such future refinements.

We demonstrate that by mode selective excitation of the various fundamentals it is possible to selectively promote or inhibit the stereomutation tunneling rate, compared to the one in the vibrational ground state.

Hydrogen ditelluride as well as $HOClH^+$ are interesting cases for such investigations and for a systematic comparison with the other members of the above mentioned series. For example, the *trans* torsional electronic potential barrier height for H_2Te_2 ($V_{el,trans}(H_2Te_2)$) = 1780 cm^{-1} is comparable to the one of H_2Se_2 ($V_{el,trans}(H_2Se_2)$ = 1672 cm^{-1}), however, the corresponding tunneling splittings are much smaller than those of H_2Se_2. In a simple picture this has two reasons: (i) the broader and somewhat higher torsional barriers in H_2Te_2, and (ii) the higher effective reduced torsional moments of inertia, which is caused by the longer H–Te bond length compared to the H–Se bond length. A corresponding comparison for $HOClH^+$ ion with the isoelectronic HSOH shows that the value for the vibrational ground state tunneling splitting of HSOH is one order of magnitude smaller than that of the $HOClH^+$ ion, which can be explained by the larger *trans* torsional barrier height of $V_{el,trans}(HSOH)$ = 1473 cm^{-1} compared with $V_{el,trans}(HClOH^+)$ = 1180 cm^{-1}. (In this case the H–Cl bond length (130.5 pm) in the $HOClH^+$ ion is very similar to the H–S bond length (134.5 pm) in HSOH and therefore the effective torsional moments are more or less the same.)

Our predictions may provide a motivation for a first synthesis of the $HClOH^+$ ion under mass spectroscopic conditions and for its spectroscopic observation. Because of the high isomerization barrier of more than 1 eV towards reaction to the more stable isomer H_2OCl^+, we predict sufficient kinetic stability for $HOClH^+$ for a spectroscopic detection. The deprotonation energy of $HOClH^+$ is high as well, about 6.6 eV [36].

Our predictions should also be useful for the first study of H_2Te_2 by rotational-vibrational spectroscopy. An important motivation for the latter is our prediction of the present work that the ground state tunneling splittings are much smaller than the large values of the parity-violating potential of the order of $10^{-9}\,cm^{-1}$ [48,49]. By comparing the values of $\Delta E_{\pm}$ and ΔE_{pv} it is obvious that H_2Te_2 and especially its isotopomers are potentially useful candidates for the spectroscopic investigation of parity violation. For H_2Te_2 the values for ΔE_{pv} are predicted to be smaller than $\Delta E_{\pm}$ and thus weak parity mixing might be observable by techniques

as proposed in refs. [17,19]. However, for D_2Te_2 and T_2Te_2 ΔE_{pv} is nearly three orders to seven orders of magnitude larger than $\Delta E_{\pm}$. In this case ΔE_{pv} is a directly measurable energy difference between the ground state energies of the P and M enantiomers, which are stabilized against tunneling by parity violation. Thus ΔE_{pv} could be measured by the basic superposition technique proposed in ref. [20], for which several variants have now been discussed [19]. Indeed, D_2Te_2 is the only non-radioactive hydride isotopomer in the whole series, which satisfies the conditions for such experiments. In particular a complete realization of this experiment in the infrared range would be possible, for which our calculations of the corresponding infrared tunneling spectra are of the highest significance. Of course, also the approaches using parity violating frequency shifts (without measuring ΔE_{pv}) could be used [14,15,29–31,70] and we plan also calculations for such frequency shifts particularly for the D_2Te_2 isotopomer, where these could be experimentally relevant. Given the particular spectroscopic simplicity of this compound, it may thus serve one day as prototypical for spectroscopic measurements of parity violation as it is prototypical in neutralization–reionization mass spectroscopy [71]. In any case the present paper has herewith identified the first non-radioactive hydride of this type of relevance for measurements of ΔE_{pv}. Of course, also non hydrides such as Cl_2S_2 deserve attention [26].

Also our results on $HOClH^+$ can be considered to be prototypical for ions, as we herewith present the first case of an ion in this series, where predictions for parity violation and tunneling are available. It is obvious from our results and the summary in Table 11, that $HOClH^+$ is not a suitable candidate for observing molecular (ionic) parity violation, because its dynamics is dominated by tunneling. The simple systematic trends in comparison with the isoelectronic HSOH [27] indicate that also for the corresponding ions analogous to the heaviest members of the series in Table 11 parity violation will dominate over tunneling. Certainly, the present systematic investigation indicates that a further investigation of molecular ions of the type $HTeIH^+$ or $HTeBrH^+$, etc. deserves attention, even though the advantages of using molecular ions for spectroscopic investigations of parity violation [44] may well be counterbalanced by similarly large or larger disadvantages compared to neutrals [19,20,45]. But at the present stage, it is certainly appropriate to pursue exploratory efforts in several directions at the same time (see also [76]).

The systematic behavior revealed by our results in Table 11 is also of more general interest. It clearly indicates that by systematic variations in series of related molecules it is possible to finetune the size of parity violation and tunneling energies in such a way as to optimize molecular properties for spectroscopic investigations of molecular parity violation and to our knowledge Table 11 is the first example of presenting a fairly complete set with a clear positive result in terms of the properties of D_2Te_2.

Acknowledgements

Many years of friendly scientific exchange with Tilmann Märk are gratefully acknowledged. Our work is supported financially by the ETH Zürich and the Schweizerischer Nationalfonds (including C4 and CSCS). We enjoyed fruitful discussions with Robert Berger, Sofia Deloudi, David Luckhaus and Achim Sieben.

References

[1] T. Karl, A. Hansel, T.D. Märk, W. Lindinger, D. Hoffmann, Int. Mass Spectrom. 223 (2003) 527.
[2] F. Biasoli, F. Gasperi, E. Aprea, E. Boscaini, T.D. Märk, Int. Mass Spectrom. 223 (2003) 343.
[3] C. Lifshitz, T.D. Märk, Ionization Theory in Encyclopedia of Spectroscopy, Academic Press, London, 1999, p. 1010.
[4] T.D. Märk, Int. J. Mass Spectrom. Ion Phys. 45 (1982) 125.
[5] T.D. Märk, Book Electron–Molecule Interactions and their Applications, vol. 1, Academic Press, London, 1999, Chapter 3, p. 251.
[6] T.D. Märk, J.A.W. Castleman, Exp. Stud. Cluster Ions, Adv. Atom. Mol. Phys. 20 (1985) 65.
[7] T.D. Märk, P. Scheier, J. Chem. Phys. 87 (1987) 1456.
[8] O. Echt, T.D. Märk, Cluster and Cluster Ions in Encyclopedia of Spectroscopy, Academic Press, London, 1999, p. 327.
[9] T.D. Märk, M. Foltin, P. Scheier, in: M. Bremer, T. Lönnroth, F.B. Mulik (Eds.), Clustering Phenomena in Atoms and Nuclei, Springer, Berlin, 1992, p. 313.
[10] M. Foltin, M. Lezius, P. Scheier, T.D. Märk, J. Chem. Phys. 98 (1993) 9624.
[11] M. Hippler, M. Quack, R. Schwarz, G. Seyfang, S. Matt, T. Märk, Chem. Phys. Lett. 278 (1997) 111.
[12] M. Quack, Angew. Chem. Int. Ed. (Engl.) 28 (1989) 571.
[13] M. Quack, Nova Acta Leopoldina N.F. 81 (1999) 137.
[14] V.S. Letokhov, Phys. Lett. A 53 (1975) 275.
[15] E. Arimondo, P. Glorieux, T. Oka, Opt. Commun. 23 (1977) 369.
[16] B.Y. Zeldovich, D.B. Saakyan, I.I. Sobelman, Soviet. Phys. JETP Lett. 25 (1977) 94.
[17] R.A. Harris, L. Stodolski, Phys. Lett. B 78 (1978) 313.
[18] R.A. Hegstrom, D.W. Rein, P.G.H. Sandars, J. Chem. Phys. 73 (1980) 2329.
[19] M. Quack, Angew. Chem. Intl. Ed. (Engl.) 114 (2002) 4812.
[20] M. Quack, Chem. Phys. Lett. 132 (1986) 147.
[21] A. Bakasov, T.K. Ha, M. Quack, in: J. Chela-Flores, F. Rolin (Eds.), Proceedings of the 4th Trieste Conference (1995), Chemical Evolution: Physics of the Origin and Evolution of Life, Kluwer Academic Publishers, Dordrecht, 1996, p. 287.
[22] A. Bakasov, T.K. Ha, M. Quack, J. Chem. Phys. 109 (1998) 7263.
[23] A. Bakasov, M. Quack, Chem. Phys. Lett. 303 (1999) 547.
[24] R. Berger, M. Quack, J. Chem. Phys. 112 (2000) 3148.
[25] M. Gottselig, D. Luckhaus, M. Quack, J. Stohner, M. Willeke, Helv. Chim. Acta 84 (2001) 1846.
[26] R. Berger, M. Gottselig, M. Quack, M. Willeke, Angew. Chem. Intl. Ed. (Engl.) 40 (2001) 4195.
[27] M. Quack, M. Willeke, Helv. Chim. Acta 86 (2003) 1641.
[28] M. Quack, Chimia 57 (2003) 147.
[29] M. Quack, J. Stohner, Chirality 13 (2001) 745.
[30] M. Quack, J. Stohner, Phys. Rev. Lett. 84 (2000) 3807.
[31] M. Quack, J. Stohner, J. Chem. Phys. 119 (2003) 11228.
[32] R. Berger, M. Quack, A. Sieben, M. Willeke, Helv. Chim. Acta 86 (2003) 4048.
[33] M. Gottselig, M. Quack, M. Willeke, Isr. J. Chem. (2004), in press.
[34] Y. Takeoka, N. Yasuda, in: Proceedings of International Ion Engineering Congress—ISIAT 83 and IPAT 83, 1983, p. 993.

[35] J.J. BelBruno, Heteroatom Chem. 8 (1997) 199.
[36] J.S. Francisco, S.P. Sander, J. Chem. Phys. 192 (1995) 9615.
[37] M. Manuel, O. Mó, M. Yáez, J. Mol. Struc. (Theochem.) 398 (1997) 417.
[38] M.N. Glukhovtsev, A. Pross, L. Radom, J. Phys. Chem. 100 (1996) 3498.
[39] T.K. Ghanty, S. Ghosh, J. Phys. Chem. 101 (1997) 5022.
[40] M. Iraqi, H. Schwarz, Chem. Phys. Lett. 221 (1994) 359.
[41] G. Winnewisser, F. Lewen, S. Thorwirth, M. Behnke, J. Hahn, J. Gauss, E. Herbst, Chem. Eur. J. 9 (2003) 5501.
[42] B. Fehrensen, D. Luckhaus, M. Quack, Z. Phys. Chem. N.F. 209 (1999) 1.
[43] B. Fehrensen, D. Luckhaus, M. Quack, Chem. Phys. Lett. 300 (1999) 312.
[44] V.S. Letokhov, Ber. Bunsenges. Phys. Chem. 99 (1995) 498.
[45] M. Quack, Private communication to V.S. Letokhov, 1995.
[46] S.A. Awad, J. Phys. Chem. 66 (1962) 890.
[47] C. Hop, M.A. Medina, J. Am. Chem. Soc. 116 (1994) 3163.
[48] L. Wiesenfeld, Mol. Phys. 64 (1988) 739.
[49] J.K. Laerdahl, P. Schwerdtfeger, Phys. Rev. A 60 (1999) 4439.
[50] M.J. Frisch, G.W. Trucks, H.B. Schlegel, G.E. Scuseria, M.A. Robb, J.R. Cheeseman, V.G. Zakrzewski, J.A. Montgomery, R.E. Stratmann, J.C. Burant, S. Dapprich, J.M. Millam, A.D. Daniels, K.N. Kudin, M.C. Strain, O. Farkas, J. Tomasi, V. Barone, M. Cossi, R. Cammi, B. Mennucci, C. Pomelli, C. Adamo, S. Clifford, J. Ochterski, G.A. Petersson, P.Y. Ayala, Q. Cui, K. Morokuma, D.K. Malick, A.D. Rabuck, K. Raghavachari, J.B. Foresman, J. Cioslowski, J.V. Ortiz, A.G. Baboul, B.B. Stefanov, G. Liu, A. Liashenko, P. Piskorz, I. Komaromi, R. Gomperts, R.L. Martin, D.J. Fox, T. Keith, M.A. Al-Laham, C.Y. Peng, A. Nanayakkara, M. Challacombe, P.M.W. Gill, B.G. Johnson, W. Chen, M.W. Wong, J.L. Andres, C. Gonzalez, M. Head-Gordon, E.S. Replogle, J.A. Pople, Gaussian 98, Revision A.9, Gaussian, Inc., Pittsburgh, PA.
[51] W.R. Wadt, P.J. Hay, J. Chem. Phys. 82 (1985) 284.
[52] A. Bergner, M. Dolg, W. Kuechle, H. Stoll, H. Preuss, Mol. Phys. 80 (1993) 1431.
[53] J.M.L. Martin, A. Sundermann, J. Chem. Phys. 114 (2001) 3408.
[54] T. Cvitaš, J. Frey, B. Holmström, K. Kuchitsu, R. Marquardt, I. Mills, F. Pavese, M. Quack, J. Stohner, H.L. Strauss, M. Takami, A.J. Thor, Quantities, Units and Symbols in Physical Chemistry, IUPAC, 2004, in preparation.
[55] T. Helgaker, H.J. Jensen, P. Joergensen, J. Olsen, K. Ruud, H. Aagren, T. Andersen, K.L. Bak, V. Bakken, O. Christiansen, P. Dahle, E.K. Dalskov, T. Enevoldsen, B. Fernandez, H. Heiberg, H. Hettema, D. Jonsson, S. Kirpekar, R. Kobayashi, H. Koch, K.V. Mikkelsen, P. Norman, M.J. Packer, T. Saue, P.R. Taylor, O. Vahtras, Dalton Release 1.0 (1997), an Electronic Structure Program.
[56] R. Berger, M. Quack, J. Stohner, Angew. Chem. Intl. Ed. (Engl.) 40 (2001) 1667.
[57] R. Berger, M. Quack, Chem. Phys. Chem. 1 (2000) 57.
[58] M. Quack, J. Stohner, Z. Physik. Chemie. 214 (2000) 675.
[59] W.H. Miller, N.C. Handy, J.E. Adams, J. Chem. Phys. 72 (1980) 99.
[60] M. Quack, J. Troe, in: P.V. Ragué Schleyer, N. Allinger, T. Clark, J. Gasteiger, P.A. Kollman, H.F. Schaefer III, P.R. Schreiner (Eds.), Encyclopedia of Computational Chemistry, vol. 4, John Wiley and Sons, 1998, p. 2708.
[61] R. Meyer, J. Chem. Phys. 52 (1970) 2053.
[62] D. Luckhaus, J. Chem. Phys. 113 (2000) 1329.
[63] B. Fehrensen, D. Luckhaus, M. Quack, M. Willeke, T. Rizzo, J. Chem. Phys. 119 (2003) 5534.
[64] B. Kuhn, T.R. Rizzo, D. Luckhaus, M. Quack, M. Suhm, J. Chem. Phys. 111 (1999) 2565.
[65] D.W. Lupo, M. Quack, Chem. Rev. 87 (1987) 181.
[66] K.V. Puttkamer, M. Quack, Chem. Phys. 139 (1989) 31.
[67] M. Quack, in: J. Jortner, R.D. Levine, B. Pullman (Eds.), Mode Selective Chemistry, Kluwer Academic Publishers, Dordrecht, 1991, p. 47.
[68] F.F. Crim, Annu. Rev. Phys. Chem. 44 (1993) 397.
[69] M. Quack, Annu. Rev. Phys. Chem. 41 (1990) 839.
[70] C. Daussy, T. Marrel, A. Amy-Klein, C.T. Nguyen, C.J. Borde, C. Chardonnet, Phys. Rev. Lett. 83 (1999) 1554.
[71] N. Goldberg, H. Schwarz, Acc. Chem. Res. 27 (1994) 347.
[72] C.S. Ewig, E.H. Mei, J.R. van Wazer, Mol. Phys. 40 (1980) 241.
[73] R. Laitinen, T. Pakkanen, J. Mol. Struct. 25 (1985) 293.
[74] R. Block, L. Jansen, J. Chem. Phys. 82 (1985) 3322.
[75] W.B. Olson, R.H. Hunt, B.W. Young, A.G. Maki, J.W.J. Brault, J. Mol. Spectrosc. 128 (1988) 12.
[76] J. Stohner, Int. J. Mass Spectr. 233 (2004) 385.